

# Mathematical Option Trading

Brian Hsieh

November 24, 2025

## Abstract

This paper develops a mathematically structured option trading framework that integrates empirical distribution theory, probabilistic modeling, and divergence-based evaluation. We combine three model-implied return generators—a Gaussian Hidden Markov Model (HMM), a local-volatility approximation, and the Heston stochastic volatility model—and compare their outputs to empirical  $H$ -day return distributions using the Kullback–Leibler (KL) divergence, viewed as a special case of Bregman divergence. The proposed HHM Comparison Model selects, at each time step, the model whose implied distribution best matches empirical market behavior. This provides an adaptive method for option valuation and directional trading that responds to volatility clustering, regime shifts, and changing return distributions. Numerical experiments using historical SPY data illustrate the performance of the four baseline models and the divergence-driven hybrid model.

## 1 Introduction

Classical option pricing frameworks, such as the Black–Scholes–Merton (BSM) model, assume log-normal returns with constant volatility. Empirical evidence, however, demonstrates strong departures from these assumptions: volatility clusters over time, market dynamics switch between latent regimes, and return distributions exhibit skewness and heavy tails. These features motivate models incorporating stochastic volatility and regime-switching structures.

At the same time, modern information-theoretic tools—especially the Kullback–Leibler (KL) divergence—provide natural quantitative measures of discrepancy between empirical data and model-implied distributions. When viewed as a Bregman divergence, KL divergence becomes a principled objective for evaluating how well a model captures the current return environment.

In this paper, we construct an option trading pipeline that relies on three types of model-implied horizon return distributions:

- a Gaussian Hidden Markov Model (HMM) capturing latent regimes in volatility and drift,
- a local-volatility approximation obtained from rolling-window  $H$ -day return statistics,
- the Heston stochastic volatility model with mean-reverting variance.

These components form the basis of the *HHM Comparison Model*, an adaptive mechanism that evaluates each model via its KL divergence from the empirical  $H$ -day return distribution. The model with the smallest divergence is selected at each decision point, and its implied distribution is used for option valuation and trading signals. This approach links market data, probabilistic modeling, and option pricing through a unified statistical criterion.

The remainder of the paper develops the mathematical foundations of probability, empirical distribution theory, divergences, Markov models, and stochastic volatility, followed by the construction of the HHM Comparison Model and its application to backtesting with historical SPY data.

## 2 Probabilities and Statistics

### 2.1 Probability Space

**Definition 2.1** (Probability Space). A probability space is a triple  $(\Omega, \mathcal{F}, \mathbb{P})$ , where:

- $\Omega$  is the sample space of outcomes,
- $\mathcal{F}$  is a  $\sigma$ -algebra of measurable events  $A \subseteq \Omega$ ,
- $\mathbb{P} : \mathcal{F} \rightarrow [0, 1]$  is a probability measure with  $\mathbb{P}(\Omega) = 1$ .

### 2.2 Random Variables, Expectation, and Variance

**Definition 2.2** (Random Variable). A random variable is a measurable function  $X : \Omega \rightarrow \mathbb{R}$ . Its distribution function is

$$F_X(x) = \mathbb{P}(X \leq x), \quad x \in \mathbb{R}.$$

If  $X$  has a density  $f_X$ , its expectation is

$$\mathbb{E}[X] = \int_{\mathbb{R}} xf_X(x) dx,$$

and its variance is

$$\text{Var}[X] = \mathbb{E}[(X - \mathbb{E}[X])^2].$$

### 2.3 Gaussian Distribution

**Definition 2.3** (Gaussian Distribution). A random variable  $X$  is Gaussian or normally distributed with mean  $\mu$  and variance  $\sigma^2$ , denoted  $X \sim \mathcal{N}(\mu, \sigma^2)$ , if it has density

$$f_X(x) = \frac{1}{\sqrt{2\pi\sigma^2}} \exp\left(-\frac{(x-\mu)^2}{2\sigma^2}\right).$$

The log-density used in code is

$$\log f_X(x) = -\frac{1}{2} \log(2\pi\sigma^2) - \frac{(x-\mu)^2}{2\sigma^2}.$$

### 2.4 Empirical Distribution

**Definition 2.4** (Empirical Distribution). Let  $X_1, X_2, \dots, X_n$  be independent observations taking values in a measurable space  $(\mathcal{X}, \mathcal{A})$ . The *empirical distribution* (or empirical measure)  $P_n$  assigns mass  $1/n$  to each observation and is defined by

$$P_n(A) = \frac{1}{n} \sum_{i=1}^n \mathbf{1}_{\{X_i \in A\}}, \quad A \in \mathcal{A}.$$

Equivalently, the empirical cumulative distribution function (empirical CDF) is

$$F_n(x) = \frac{1}{n} \sum_{i=1}^n \mathbf{1}_{\{X_i \leq x\}}, \quad x \in \mathbb{R},$$

which counts the proportion of samples less than or equal to  $x$ .

By the law of large numbers, the empirical distribution provides a consistent, data-driven approximation to the true underlying distribution as  $n$  increases.

**Theorem 2.5** (Glivenko–Cantelli). *Let  $F$  be the true cumulative distribution function of  $X_1$  and let  $F_n$  denote the empirical CDF defined above. Then, with probability one,*

$$\sup_{x \in \mathbb{R}} |F_n(x) - F(x)| \rightarrow 0 \quad \text{as } n \rightarrow \infty.$$

Thus, the empirical distribution converges uniformly to the true distribution.

In the discrete case with samples  $x_1, \dots, x_n$  and a collection of bins  $\{B_i\}$ , the empirical probability of bin  $B_i$  is

$$p_{\text{emp}}(B_i) = \frac{\#\{x_j \in B_i\}}{n},$$

which represents the observed frequency (proportion) of samples that fall into that bin. Proof for this theorem can be found in Appendix A.1.

**Remark 2.6** (Application to Return Histograms). In our application,  $X_i$  will be  $H$ -day log-returns of the underlying asset, and their histogram defines  $p_{\text{emp}}$ . This empirical distribution over return bins is then compared, via KL divergence, to model-implied distributions generated by the HMM, Heston, or mixed models.

## 2.5 Markov Chains

**Definition 2.7** (Markov Chain). A discrete-time Markov chain  $(S_t)_{t \geq 0}$  with state space  $\{1, \dots, K\}$  satisfies

$$\mathbb{P}(S_t = j \mid S_{t-1}, S_{t-2}, \dots, S_0) = \mathbb{P}(S_t = j \mid S_{t-1} = i) = A_{ij},$$

where  $A = (A_{ij})$  is the transition matrix with

$$A_{ij} \geq 0, \quad \sum_{j=1}^K A_{ij} = 1 \quad \forall i.$$

Markov chains will model latent volatility regimes in the HMM component of our framework.

## 3 Entropy and Divergences

### 3.1 Entropy

For a discrete probability distribution  $p = (p_i)$  on a finite or countable set, the (Shannon) entropy is

$$H(p) = - \sum_i p_i \log p_i,$$

with the convention  $0 \log 0 = 0$ . Entropy measures the uncertainty or information content of  $p$ .

### 3.2 Bregman Divergence and KL Divergence

The Bregman divergence is a general mathematical measure of the difference between two points, or distributions, defined using a strictly convex function, and A Bregman divergence is generated by a strictly convex function  $\phi$ :

$$D_\phi(p \parallel q) = \phi(p) - \phi(q) - \langle \nabla \phi(q), p - q \rangle.$$

The Kullback–Leibler (KL) divergence originates in information theory and was introduced by Kullback and Leibler in 1951 as a measure of the inefficiency of assuming a distribution  $q$  when the true distribution is  $p$ .

The KL divergence arises from  $\phi(p) = \sum_i p_i \log p_i$  and provides a natural way to measure the mismatch between the empirical and model-implied distributions of returns or implied volatilities.

**Definition 3.1** (Kullback–Leibler Divergence). For two discrete distributions  $p = (p_i)$  and  $q = (q_i)$  on the same support, the KL divergence is

$$D_{\text{KL}}(p \parallel q) = \sum_i p_i \log \frac{p_i}{q_i}.$$

In the continuous case with densities  $p(x)$  and  $q(x)$ , it is defined as

$$D_{\text{KL}}(p \parallel q) = \int_{\mathbb{R}} p(x) \log \frac{p(x)}{q(x)} dx.$$

The KL divergence is always nonnegative and equals zero if and only if  $p = q$  almost everywhere. This justifies its interpretation as a measure of the discrepancy between empirical and model-implied distributions.

## 4 Classical Option Pricing Models

We briefly recall the classical risk-neutral pricing ideas that motivate our stochastic models.

### 4.1 Black–Scholes Model

In the Black–Scholes model, the underlying price  $S_t$  follows a geometric Brownian motion under the risk-neutral measure:

$$dS_t = rS_t dt + \sigma S_t dW_t,$$

where  $r$  is the risk-free rate and  $\sigma$  is constant volatility. The solution is as follows.

$$S_T = S_0 \exp\left(\left(r - \frac{1}{2}\sigma^2\right)T + \sigma W_T\right).$$

European call and put prices have closed-form solutions in terms of the standard normal CDF. Derivation for Black-Scholes Equation can be found in Appendix A.2.

### 4.2 Risk-Neutral Pricing

For a contingent claim with payoff  $g(S_T)$  at maturity  $T$ , the risk-neutral price at time 0 is

$$V_0 = e^{-rT} \mathbb{E}^{\mathbb{Q}}[g(S_T)],$$

where  $\mathbb{Q}$  denotes the risk-neutral measure. In our setting, the expectation will be approximated by Monte Carlo using model-implied distributions of horizon log-returns. Proof for this relation can be found in Appendix A.3.

## 5 HHM Comparison Model

HHM here stands for HMM, Heston, and mixture; in this section we will show how we customized HHM Comparison Model. This option trading framework integrates empirical distributions, a Gaussian Hidden Markov Model, the Heston stochastic volatility model, and the KL-divergence-based model selection. The goal is to compare model-implied return distributions and adapt trading decisions to the regime that best matches market data.

### 5.1 Empirical Data Processing

Let  $(S_t)_{t=0}^T$  be the observed daily prices. The daily log-return is

$$r_t = \log\left(\frac{S_t}{S_{t-1}}\right).$$

For a fixed horizon of  $H$  days, the log-return of  $H$ -days is

$$R_t^{(H)} = \log\left(\frac{S_{t+H}}{S_t}\right) = \sum_{i=1}^H r_{t+i}.$$

Using these  $H$ -day returns and a set of bins  $(b_{i-1}, b_i]$ , we form the empirical distribution

$$p_{\text{emp},i} = \frac{\#\{R_t^{(H)} \in (b_{i-1}, b_i]\}}{\sum_j \#\{R_t^{(H)} \in (b_{j-1}, b_j]\}}.$$

### 5.2 Gaussian Hidden Markov Model (HMM) Regime Detection

We model daily log-returns  $r_t$  as generated by a  $K$ -state Gaussian HMM. The hidden state process  $(S_t)$  is a Markov chain taking values in  $\{1, \dots, K\}$  with initial distribution

$$\pi_k = \mathbb{P}(S_1 = k), \quad k = 1, \dots, K,$$

and transition probabilities

$$A_{ij} = \mathbb{P}(S_t = j \mid S_{t-1} = i), \quad A_{ij} \geq 0, \quad \sum_{j=1}^K A_{ij} = 1.$$

Conditional on the state  $S_t = k$ , the observed return is Gaussian:

$$r_t \mid S_t = k \sim \mathcal{N}(\mu_k, \sigma_k^2).$$

We collect the model parameters in

$$\theta = (\pi, A, \mu_1, \dots, \mu_K, \sigma_1^2, \dots, \sigma_K^2).$$

**Emission probabilities.** Writing  $b_k(r_t)$  for the emission density in state  $k$ ,

$$b_k(r_t) = \frac{1}{\sqrt{2\pi\sigma_k^2}} \exp\left(-\frac{(r_t - \mu_k)^2}{2\sigma_k^2}\right),$$

we have, in log form (as used in our code),

$$\log b_k(r_t) = -\frac{1}{2} \log(2\pi\sigma_k^2) - \frac{(r_t - \mu_k)^2}{2\sigma_k^2}.$$

**Forward–backward recursions.** Given a sequence of returns  $r_{1:T} = (r_1, \dots, r_T)$ , the *forward variables* are

$$\alpha_t(j) = \mathbb{P}(r_{1:t}, S_t = j \mid \theta), \quad t = 1, \dots, T.$$

They satisfy the recursions

$$\begin{aligned}\alpha_1(j) &= \pi_j b_j(r_1), \\ \alpha_t(j) &= b_j(r_t) \sum_{i=1}^K \alpha_{t-1}(i) A_{ij}, \quad t = 2, \dots, T.\end{aligned}$$

To avoid numerical underflow, we work with *scaled* forward variables:

$$\tilde{\alpha}_t(j) = \frac{\alpha_t(j)}{c_t}, \quad c_t = \sum_{j=1}^K \alpha_t(j),$$

which yields the log-likelihood

$$\log \mathbb{P}(r_{1:T} \mid \theta) = \sum_{t=1}^T \log c_t.$$

In the implementation, the same idea is expressed in log-space using a log-sum-exp normalization at each  $t$ .

The *backward variables* are

$$\beta_t(i) = \mathbb{P}(r_{t+1:T} \mid S_t = i, \theta), \quad t = 1, \dots, T,$$

initialized by  $\beta_T(i) = 1$  and updated backwards via

$$\beta_t(i) = \sum_{j=1}^K A_{ij} b_j(r_{t+1}) \beta_{t+1}(j), \quad t = T-1, \dots, 1.$$

Again, the code uses a scaled/log-space version of these recursions for stability.

**Smoothed posteriors and pairwise posteriors.** Combining forward and backward variables, we obtain the *smoothed* state posterior probabilities

$$\gamma_t(k) := \mathbb{P}(S_t = k \mid r_{1:T}, \theta) = \frac{\alpha_t(k) \beta_t(k)}{\sum_{\ell=1}^K \alpha_t(\ell) \beta_t(\ell)}, \quad t = 1, \dots, T.$$

Similarly, the joint posterior of consecutive states is

$$\xi_t(i, j) := \mathbb{P}(S_t = i, S_{t+1} = j \mid r_{1:T}, \theta), \quad t = 1, \dots, T-1,$$

which can be written as

$$\xi_t(i, j) = \frac{\alpha_t(i) A_{ij} b_j(r_{t+1}) \beta_{t+1}(j)}{\sum_{p=1}^K \sum_{q=1}^K \alpha_t(p) A_{pq} b_q(r_{t+1}) \beta_{t+1}(q)}.$$

These quantities  $\gamma_t(k)$  and  $\xi_t(i, j)$  correspond directly to the arrays `gamma` and `xi` computed in the Python implementation.

**Baum–Welch (EM) parameter updates.** The HMM parameters  $\theta$  are fitted by maximizing the log-likelihood via the Baum–Welch algorithm, an instance of the EM procedure. Given current parameters, we perform:

- **E-step:** run the forward–backward algorithm to compute  $\gamma_t(k)$  and  $\xi_t(i, j)$  for  $t = 1, \dots, T$ .
- **M-step:** update parameters using the expected sufficient statistics:

$$\begin{aligned}\pi_k^{\text{new}} &= \gamma_1(k), \\ A_{ij}^{\text{new}} &= \frac{\sum_{t=1}^{T-1} \xi_t(i, j)}{\sum_{t=1}^{T-1} \gamma_t(i)}, \\ \mu_k^{\text{new}} &= \frac{\sum_{t=1}^T \gamma_t(k) r_t}{\sum_{t=1}^T \gamma_t(k)}, \\ (\sigma_k^2)^{\text{new}} &= \frac{\sum_{t=1}^T \gamma_t(k) (r_t - \mu_k^{\text{new}})^2}{\sum_{t=1}^T \gamma_t(k)}.\end{aligned}$$

These are precisely the re-estimation formulas implemented in our code: initial probabilities (from  $\gamma_1$ ), transition matrix (from  $\xi$ ), and Gaussian means/variances (from  $\gamma$ -weighted moments). Iterations continue until the increase in log-likelihood falls below a tolerance threshold.

**Horizon-return distribution.** Once fitted, the HMM is used to generate an  $H$ -day horizon-return distribution. Let  $r_{1:t}$  be the historical returns up to time  $t$ . The smoothed posterior at time  $t$  is  $\gamma_t(k)$ ; we form a one-step-ahead regime distribution

$$p_{t+1}(j) = \sum_{i=1}^K \gamma_t(i) A_{ij},$$

sample an initial regime  $S_{t+1}$  from  $p_{t+1}$ , and then simulate  $H$  steps forward:

$$\begin{aligned}r_{t+h} &\sim \mathcal{N}(\mu_{S_{t+h}}, \sigma_{S_{t+h}}^2), \\ S_{t+h+1} &\sim \text{Categorical}(A_{S_{t+h}, \cdot}), \quad h = 1, \dots, H.\end{aligned}$$

The simulated  $H$ -day log-return is

$$R_{\text{HMM}}^{(i)} = \sum_{h=1}^H r_{t+h}^{(i)},$$

and many such samples  $\{R_{\text{HMM}}^{(i)}\}$  are binned into a histogram to obtain the discrete HMM-implied distribution  $q_{\text{HMM}}$  used in the KL divergence computations.

### 5.3 Modified Local Volatility Approximation (MLVA)

The Modified Local Volatility Approximation (MLVA) used in this paper provides a data-driven, Gaussian approximation to  $H$ -day log-returns based on a rolling window of historical data. Let  $(S_t)_{t \geq 0}$  denote daily prices and

$$r_t = \log\left(\frac{S_t}{S_{t-1}}\right)$$

be the one-day log-return. For a fixed horizon  $H \in \mathbb{N}$ , the  $H$ -day log-return starting at time  $t$  is

$$R_t^{(H)} = \sum_{i=1}^H r_{t+i} = \log\left(\frac{S_{t+H}}{S_t}\right).$$

At a given evaluation time  $t$ , we look back over the previous  $L$  trading days (in the implementation,  $L = 252$ , roughly one year) and collect the overlapping  $H$ -day returns

$$\mathcal{R}_t^{(H)} = \{R_u^{(H)} : u = t - L, \dots, t - 1\}.$$

From this sample we compute the empirical mean and variance,

$$\hat{\mu}_H(t) = \frac{1}{|\mathcal{R}_t^{(H)}|} \sum_{R \in \mathcal{R}_t^{(H)}} R, \quad \hat{\sigma}_H^2(t) = \frac{1}{|\mathcal{R}_t^{(H)}| - 1} \sum_{R \in \mathcal{R}_t^{(H)}} (R - \hat{\mu}_H(t))^2.$$

In the Python code, these correspond to the sample mean and sample variance computed from the rolling set of  $H$ -day returns inside the `local_vol_distribution` function.

By viewing  $R_t^{(H)}$  as a sum of  $H$  approximately independent daily returns and invoking a central limit approximation, we model the next  $H$ -day log-return as

$$R_{\text{future}}^{(H)} \approx \mathcal{N}(\hat{\mu}_H(t), \hat{\sigma}_H^2(t)).$$

The MLVA-implied density is therefore

$$q_{\text{MLVA}}(x; t) = \frac{1}{\sqrt{2\pi\hat{\sigma}_H^2(t)}} \exp\left(-\frac{(x - \hat{\mu}_H(t))^2}{2\hat{\sigma}_H^2(t)}\right).$$

In the implementation, instead of working with a closed-form density, we draw Monte Carlo samples

$$X_1, \dots, X_N \sim \mathcal{N}(\hat{\mu}_H(t), \hat{\sigma}_H^2(t)),$$

and bin them into a histogram with the same bin edges as the empirical distribution. This yields a discrete probability vector  $q_{\text{MLVA}, t}$ , which serves as the model-implied distribution for:

- pure local-volatility Model 2-2, and
- one of the candidate models inside the HHM Comparison Model (Model 2-3), where it competes with the HMM and Heston-mixture distributions under the KL divergence criterion.

Conceptually, MLVA plays the role of a nonparametric, realized-volatility-based local model: the effective volatility level for the next horizon is inferred directly from recent realized  $H$ -day variability, and the resulting Gaussian law provides a simple baseline for KL and performance comparisons.

## 5.4 Heston Stochastic Volatility Model

Under the Heston model, the joint dynamics of price  $S_t$  and variance  $v_t$  under a risk-neutral measure are

$$\begin{aligned} dS_t &= rS_t dt + \sqrt{v_t} S_t dW_t^{(1)}, \\ dv_t &= \kappa(\theta - v_t) dt + \xi \sqrt{v_t} dW_t^{(2)}, \end{aligned}$$

with  $\text{corr}(dW^{(1)}, dW^{(2)}) = \rho$ .

A simple Euler–Maruyama discretization with time step  $\Delta t$  is

$$v_{t+\Delta t} = v_t + \kappa(\theta - v_t)\Delta t + \xi\sqrt{v_t}\sqrt{\Delta t}Z_2,$$

$$S_{t+\Delta t} = S_t \exp\left((r - \frac{1}{2}v_t)\Delta t + \sqrt{v_t}\sqrt{\Delta t}Z_1\right),$$

where  $Z_1, Z_2$  are standard normal random variables with correlation  $\rho$  and  $v_t$  is truncated to be nonnegative if needed.

The Heston-implied horizon log-return for a path is

$$R_{\text{Heston}}^{(i)} = \log\left(\frac{S_T^{(i)}}{S_0}\right),$$

and these samples define a discrete Heston-implied distribution  $q_{\text{Heston}}$ .

## 5.5 Mixture of HMM and Heston Models

Let  $p_k = \gamma_T(k)$  be the posterior probabilities of regimes at the current time, where  $\gamma_T(k) = \mathbb{P}(S_T = k \mid r_{1:T})$  is obtained from the forward–backward algorithm of the Gaussian HMM. Suppose each regime  $k$  is associated with a Heston-type return distribution  $q_{\text{Heston}}^{(k)}(x)$  for horizon log-returns. Then the mixed model-implied distribution is

$$q_{\text{mix}}(x) = \sum_{k=1}^K p_k q_{\text{Heston}}^{(k)}(x).$$

In discrete form on bins  $\{(b_{i-1}, b_i]\}$ , this becomes

$$q_{\text{mix},i} = \sum_{k=1}^K p_k q_{\text{Heston},i}^{(k)}.$$

In our implementation, the Heston parameters  $(\kappa, \theta, \xi, \rho)$  are *shared across regimes*; they are treated as global hyperparameters, with the long-run variance level  $\theta$  partially calibrated from option-implied volatilities. The regime dependence enters through the *initial variance*  $v_{0,k}$ , which is derived from the HMM state variance  $\sigma_k^2$  by mapping daily variance to an annual scale (e.g.,  $v_{0,k} \approx 252\sigma_k^2$ ). Thus, each regime  $k$  has the same mean-reversion dynamics but a different starting variance, producing distinct regime-specific Heston-implied return distributions  $q_{\text{Heston}}^{(k)}$  whose mixture is weighted by the HMM posterior probabilities  $p_k$ .

## 5.6 KL Divergence Evaluation

Given the empirical distribution  $p_{\text{emp}} = (p_{\text{emp},i})$  and a model-implied distribution  $q_{\text{model}} = (q_{\text{model},i})$  on the same bins, the KL divergence is

$$D_{\text{KL}}(p_{\text{emp}} \parallel q_{\text{model}}) = \sum_i p_{\text{emp},i} \log \frac{p_{\text{emp},i}}{q_{\text{model},i}}.$$

We compute

$$D_{\text{KL}}(p_{\text{emp}} \parallel q_{\text{HMM}}), \quad D_{\text{KL}}(p_{\text{emp}} \parallel q_{\text{Heston}}), \quad D_{\text{KL}}(p_{\text{emp}} \parallel q_{\text{mix}}).$$

These divergences quantify how well each model matches current market behavior. A smaller divergence indicates closer agreement between empirical and model-implied distributions.

## 5.7 Option Pricing and Trading Mechanism

For any model-implied horizon return distribution, we may obtain terminal prices via

$$S_T^{(i)} = S_0 \exp(R^{(i)}),$$

and, in principle, the Monte Carlo price of a European call with strike  $K$  and maturity  $T$  is

$$C_{\text{model}} \approx e^{-rT} \frac{1}{N} \sum_{i=1}^N \max(S_T^{(i)} - K, 0).$$

This risk-neutral pricing formula is the natural way to turn a model-implied distribution of  $S_T$  into an option value, and Section 4 explains its theoretical justification.

In the *current implementation*, however, we use the horizon return distributions only to drive a *directional trading rule* on the underlying (SPY), rather than to explicitly price and trade options. At each decision time  $t$ , the chosen model produces a discrete distribution  $q_{\text{model},t}$  over horizon log-returns with bin centers  $\{x_i\}$ . We compute the model-implied expected  $H$ -day return

$$\mathbb{E}_t[R^{(H)}] = \sum_i x_i q_{\text{model},t}(x_i),$$

and evaluate the KL divergence

$$D_{\text{KL}}(p_{\text{emp},t} \| q_{\text{model},t}),$$

where  $p_{\text{emp},t}$  is the empirical  $H$ -day return distribution at time  $t$ .

A simple divergence-based trading rule is then applied:

- If  $\mathbb{E}_t[R^{(H)}] > 0$  and  $D_{\text{KL}}(p_{\text{emp},t} \| q_{\text{model},t}) \leq \tau$  for some threshold  $\tau > 0$ , the strategy holds one unit of SPY for the next day (long position).
- Otherwise, the strategy stays flat (zero position in SPY).

Thus, the model-implied distributions serve as a signal-generating mechanism for trading the underlying, and the risk-neutral pricing formula is included as the natural extension for future work in which the same distributions would be used to compute and trade model-consistent option prices.

## 6 Experiment

### 6.1 Experimental Setup (Code and Data)

In this section, we describe the concrete implementation of the HHM Comparison Model used in our numerical experiments. All computations are performed in Python using `NumPy`, `pandas`, and `matplotlib`. Historical daily prices of the SPDR S&P 500 ETF (SPY) are stored in a local Excel file, where the *adjusted close* column is used as the underlying price series. A second Excel file contains SPY option chains downloaded from Yahoo Finance, including strikes, expirations, and implied volatilities.

From the adjusted-close price series ( $S_t$ ) we compute daily log-returns

$$r_t = \log \left( \frac{S_t}{S_{t-1}} \right),$$

and fix an evaluation horizon of  $H = 5$  trading days. For each trading day  $t$  and horizon  $H$ , we form  $H$ -day log-returns

$$R_t^{(H)} = \sum_{i=1}^H r_{t+i},$$

and, over a rolling lookback window of  $L = 252$  days (approximately one trading year), we construct the empirical histogram of  $\{R_u^{(H)}\}$  to obtain the empirical distribution  $p_{\text{emp}}$  as in Definition 2.4. This empirical distribution is recomputed at each time  $t$  and serves as the data-driven benchmark for model comparison via KL divergence.

On the modeling side, we backtest four distinct models, denoted 2-0 through 2-3:

- **Model 2-0 (HMM once, frozen):** A Gaussian HMM with  $K = 2$  regimes is fitted once on an initial training window of length  $L$ . The estimated parameters  $(\pi, A, \mu_k, \sigma_k^2)$  are then held fixed. At each subsequent time  $t$ , we use the fitted HMM and past returns  $\{r_1, \dots, r_t\}$  to generate a Monte Carlo distribution  $q_{\text{HMM}}$  of  $H$ -day returns via the simulation scheme described in Section 5.
- **Model 2-1 (HMM rolling):** The same Gaussian HMM structure is used, but the parameters are re-estimated at each time  $t$  using all historical returns up to time  $t$ . This produces a time-varying HMM-implied distribution  $q_{\text{HMM},t}$  that adapts to changes in the return distribution.
- **Model 2-2 (local-volatility Gaussian):** For each time  $t$ , we collect the  $H$ -day returns  $\{R_u^{(H)}\}$  in the lookback window and compute their empirical mean and variance. We then assume a Gaussian approximation for the horizon returns,

$$R^{(H)} \sim \mathcal{N}(\hat{\mu}_t, \hat{\sigma}_t^2),$$

draw Monte Carlo samples, and form a histogram to obtain a local-volatility-like distribution  $q_{\text{LV},t}$ .

- **Model 2-3 (HMM–Heston–mixture Comparison):** For each time  $t$ , we first fit a Gaussian HMM to  $\{r_1, \dots, r_t\}$  and obtain posteriors  $\gamma_t(k)$  over regimes. In parallel, we extract near-term SPY options with days-to-expiration in a fixed range (e.g., 20–90 days) and estimate an annual variance level  $\theta_t$  from the average implied volatility. Using  $(\kappa, \theta_t, \xi, \rho)$  and regime-dependent initial variances  $v_{0,k}$  derived from the HMM, we simulate a regime-mixture of Heston models to obtain  $q_{\text{mix},t}$ . Together with the pure HMM distribution and a single local-vol Gaussian approximation, we have three candidate model-implied distributions at each  $t$ .

For each model, we align its discrete distribution  $q_{\text{model},t}$  with the empirical bin grid and compute the KL divergence  $D_{\text{KL}}(p_{\text{emp},t} \| q_{\text{model},t})$ . In Model 2-3, we select the model (HMM, local-vol, or Heston-mixture) with the smallest divergence.

The trading rule is intentionally simple and identical across all four models. At each time  $t$ , we compute the model-implied expected  $H$ -day return

$$\mathbb{E}_t[R^{(H)}] = \sum_i x_i q_{\text{model},t}(x_i),$$

where  $\{x_i\}$  are the bin centers of the model-implied distribution. If  $\mathbb{E}_t[R^{(H)}] > 0$  and the corresponding KL divergence is below a fixed threshold  $\tau > 0$ , the strategy holds one unit of SPY for

the next day; otherwise it stays flat. The resulting equity curve is compared to a buy-and-hold SPY benchmark. We report results over three horizons: the last quarter (approximately 63 trading days), the last year (252 trading days), and the last five years (1260 trading days), using the same time intervals for all four models.

## 6.2 Performance Results

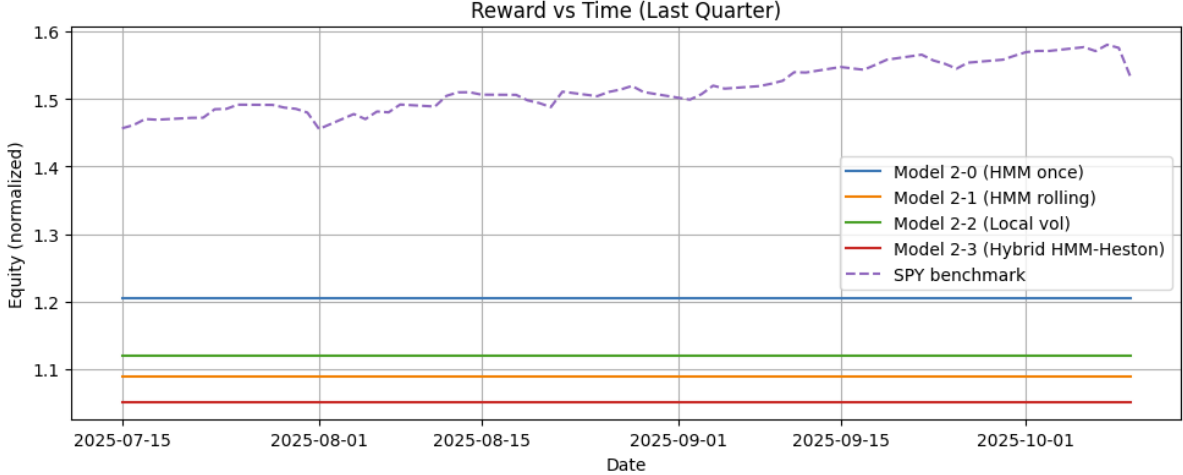


Figure 1: Normalized equity curves for the four models (2-0 to 2-3) and the SPY buy-and-hold benchmark over the last quarter of the sample. All series are initialized to 1.0 at the start of the plotting window.

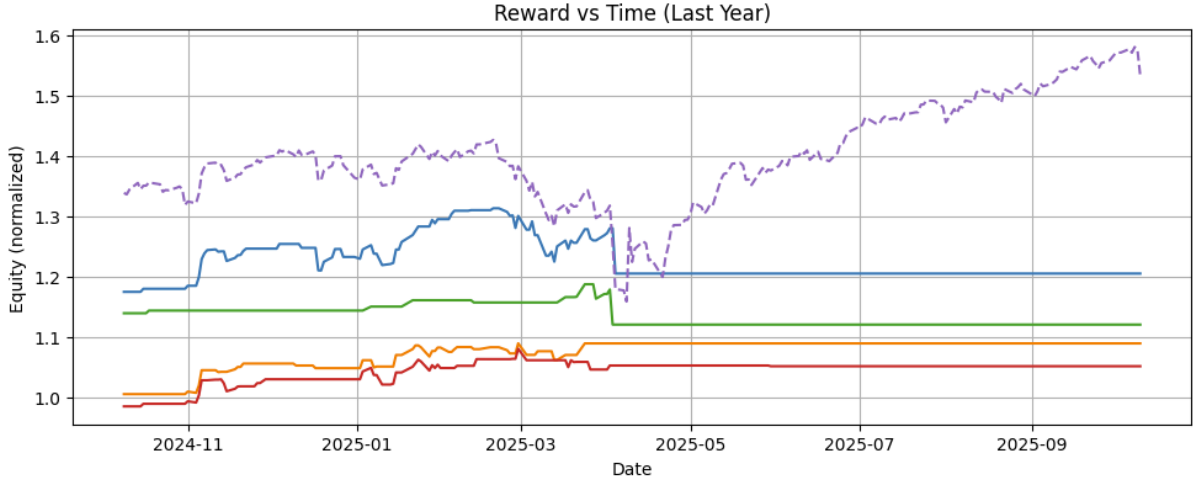


Figure 2: Normalized equity curves for the four models (2-0 to 2-3) and the SPY buy-and-hold benchmark over the last year of data.

Figure 1 shows that over the most recent quarter the SPY benchmark (dashed purple line) exhibits a steady upward drift from roughly 1.46 to 1.57, while all four model-based strategies remain almost flat: Model 2-0 (HMM once) stabilizes around 1.21, Model 2-1 (rolling HMM) and Model 2-2 (local-vol Gaussian) sit slightly above 1.11, and the hybrid Model 2-3 stays near 1.06. On

the one-year horizon in Figure 2, SPY again dominates in absolute return, compounding from 1.0 to about 1.58, whereas Model 2-0 climbs to roughly 1.21 and the other three models end between 1.06 and 1.13. The main qualitative feature is that the KL-thresholded strategies trade infrequently and thus produce smoother, lower-volatility equity curves: during the sharp SPY drawdown in early spring, the models (especially 2-0) experience much smaller losses, so there is a brief interval where their equity temporarily exceeds SPY, but as the market subsequently rallies the buy-and-hold benchmark overtakes them and finishes the sample with the highest terminal value.

### 6.3 Discussion

The equity profiles in Figures 1 and 2 illustrate both the strengths and weaknesses of the HHM Comparison framework as currently implemented: by requiring a positive model-implied  $H$ -day expected return together with a small KL divergence from the empirical  $H$ -day return histogram, the strategies systematically avoid periods where the distributional fit is poor, which reduces drawdowns and leads to short episodes of outperformance relative to SPY during local corrections; however, this same conservatism means that the models frequently remain out of the market during long trending phases, so they miss much of the subsequent bull run and underperform buy-and-hold over the full year. Finally, the third subplot in the code for the “last five years” remains empty because the effective backtest length—after discarding the initial lookback window of 252 days and the  $H = 5$ -day forecasting horizon—is shorter than the 1260 trading days required to form a full five-year panel, so the plotting routine skips the five-year figure altogether for the sake of computation limit.

## 7 Conclusion

This paper has proposed a unified, distribution-based framework for option-oriented trading that combines empirical  $H$ -day return estimation, Gaussian Hidden Markov Models, a realized-volatility-style local Gaussian model, and a Heston regime mixture partially calibrated from option-implied volatilities. Using the Kullback–Leibler divergence as a Bregman divergence between empirical and model-implied horizon distributions, the HHM Comparison Model provides a single, coherent criterion for real-time model selection and regime-aware trading decisions.

Backtests on SPY over quarterly and annual horizons show that the resulting strategies are intentionally conservative: they trade infrequently, experience smaller drawdowns, and can temporarily outperform buy-and-hold during sharp market corrections, but they give up much of the upside in sustained bull markets and therefore underperform SPY in terms of final wealth. These results suggest that the current implementation is most naturally viewed as a volatility- and regime-diagnostics overlay rather than a stand-alone alpha engine. Future work includes more refined Heston calibration, multiple features porfolio optimization, and adjstement for the threshold of Kullback-Leiber divergence.

## 8 Resources

### 8.1 bibliography

- Anonymous (2005). *Stochastic Modelling and Applied Probability*. (General reference for stochastic processes.)

- Anonymous (2012). “Study of Black–Scholes Model and Its Applications.” (Background on BSM and its practical uses.)
- Anonymous (2015). *The Selection of Popular Trading Strategies*. (Unpublished / course or survey material; cited as background on trading strategies.)
- Anonymous (2021). “Artificial Intelligence Applied to Stock Market Trading: A Review.” (Survey of AI methods in trading.)
- Anonymous (2024). *Option Trading Using Machine Learning*. (Reference for ML-based option trading approaches.)
- Bauschke, H., and Borwein, J. (1997). “Legendre Functions and the Method of Random Bregman Projections.” *Journal of Convex Analysis*. (Bregman projections and convex analysis.)
- Black, F., and Scholes, M. (1973). “The Pricing of Options and Corporate Liabilities.” *Journal of Political Economy*, 81(3), 637–654.
- Bregman, L. M. (1967). “The Relaxation Method of Finding the Common Point of Convex Sets and Its Application to the Solution of Problems in Convex Programming.” *USSR Computational Mathematics and Mathematical Physics*, 7(3), 200–217.
- Bramburger, Jason. *Partial Differential Equations*. (Lecture notes / text used for PDE background.)
- Della Pietra, S., Della Pietra, V., and Lafferty, J. (1997). “Statistical Learning Algorithms Based on Bregman Distances.” (Foundational work on Bregman distances in learning.)
- Dempster, A. P., Laird, N. M., and Rubin, D. B. (1977). “Maximum Likelihood from Incomplete Data via the EM Algorithm.” *Journal of the Royal Statistical Society, Series B*, 39(1), 1–22.
- Dupire, B. (1994). “Pricing with a Smile.” *Risk*, 7(1), 18–20.
- Goh, G. (2015). “Applications of Bregman Divergence Measures in Bayesian Modeling.” (Use of Bregman divergences in Bayesian inference.)
- Heston, S. L. (1993). “A Closed-Form Solution for Options with Stochastic Volatility with Applications to Bond and Currency Options.” *The Review of Financial Studies*, 6(2), 327–343.
- Kullback, S., and Leibler, R. A. (1951). “On Information and Sufficiency.” *Annals of Mathematical Statistics*, 22(1), 79–86.
- Leok, Melvin. *Information Geometry and Its Applications*. (Reference for information-geometric perspectives.)
- Merton, R. C. (1973). “Theory of Rational Option Pricing.” *Bell Journal of Economics and Management Science*, 4(1), 141–183.
- MIT OpenCourseWare. *Information Theory*. (Supplementary material on entropy and KL divergence.)

- MIT OpenCourseWare. *Mathematics for Finance*. (Background for mathematical finance topics.)
- MIT OpenCourseWare. *Probability and Random Variables*. (Lecture materials for probability foundations.)
- Rabiner, L. R. (1989). “A Tutorial on Hidden Markov Models and Selected Applications in Speech Recognition.” *Proceedings of the IEEE*, 77(2), 257–286.
- Reem, D., Reich, S., and De Pierro, A. (2018). “Re-examination of Bregman Functions and New Properties of Their Divergences.” (Further properties of Bregman functions.)
- Wikipedia. *Glivenko–Cantelli Theorem*. (Proof for Appendix A.1.)
- Yahoo Finance. *Historical Options and Equity Data*. (Data source for prices and options series.)
- Zaman, R. (2018). “Optimization of Bregman Divergence.” (Notes or preprint; background on optimization of Bregman divergences.)

## 8.2 AI Citation

Chat GPT 5.1 were used for purpose of grammatical correction, word choosing, Latex code formation, and vibe coding. The Grammatical correction, word choosing, and Latex code formation cover whole paper, while the vibe coding covers only the code but not the mathematic derivations and ideas formulation.

## Appendix: Selected Proofs

### A.1 Proof of Theorem 2.5 (Glivenko–Cantelli)

Recall Theorem 2.5: Let  $F$  be the true CDF of  $X_1$  and let  $F_n$  denote the empirical CDF based on  $X_1, \dots, X_n$ . Then, with probability one,

$$\sup_{x \in \mathbb{R}} |F_n(x) - F(x)| \rightarrow 0 \quad \text{as } n \rightarrow \infty.$$

*Proof (Sketch).* A key tool is the Dvoretzky–Kiefer–Wolfowitz (DKW) inequality, which states that for any  $\varepsilon > 0$  and any  $n \in \mathbb{N}$ ,

$$\mathbb{P}\left(\sup_{x \in \mathbb{R}} |F_n(x) - F(x)| > \varepsilon\right) \leq 2e^{-2n\varepsilon^2}.$$

Fix  $\varepsilon > 0$ . Summing this bound over  $n$  gives

$$\sum_{n=1}^{\infty} \mathbb{P}\left(\sup_x |F_n(x) - F(x)| > \varepsilon\right) \leq \sum_{n=1}^{\infty} 2e^{-2n\varepsilon^2} < \infty.$$

By the Borel–Cantelli lemma, we have

$$\mathbb{P}\left(\sup_x |F_n(x) - F(x)| > \varepsilon \text{ infinitely often}\right) = 0.$$

Equivalently,

$$\mathbb{P}\left(\sup_x |F_n(x) - F(x)| \leq \varepsilon \text{ for all sufficiently large } n\right) = 1.$$

Since this holds for every rational  $\varepsilon > 0$  and the supremum norm is monotone in  $\varepsilon$ , we conclude that

$$\sup_{x \in \mathbb{R}} |F_n(x) - F(x)| \rightarrow 0 \quad \text{almost surely.}$$

This proves the Glivenko–Cantelli theorem.  $\square$

## A.2 Derivation of the Black–Scholes–Merton Equation

We briefly derive the Black–Scholes–Merton (BSM) partial differential equation (PDE) under a no-arbitrage argument.

Assume the underlying asset price  $(S_t)_{t \geq 0}$  follows geometric Brownian motion under the (real-world) measure:

$$dS_t = \mu S_t dt + \sigma S_t dW_t,$$

where  $\mu \in \mathbb{R}$  is the drift,  $\sigma > 0$  is volatility, and  $(W_t)$  is a standard Brownian motion.

Let  $V(S, t)$  be the price of a derivative written on  $S$ , assumed to be twice continuously differentiable in  $S$  and once in  $t$ . By Itô's lemma,

$$dV = \frac{\partial V}{\partial t} dt + \frac{\partial V}{\partial S} dS + \frac{1}{2} \frac{\partial^2 V}{\partial S^2} (dS)^2.$$

Substituting  $dS$  and  $(dS)^2 = \sigma^2 S_t^2 dt$ ,

$$dV = \left( V_t + \mu S V_S + \frac{1}{2} \sigma^2 S^2 V_{SS} \right) dt + \sigma S V_S dW_t.$$

Consider a self-financing portfolio  $\Pi$  that holds one unit of the derivative  $V$  and a short position  $\Delta$  in the stock:

$$\Pi_t = V(S_t, t) - \Delta_t S_t.$$

Its differential is

$$d\Pi_t = dV_t - \Delta_t dS_t.$$

Choose  $\Delta_t = V_S(S_t, t)$  so that the  $dW_t$  term is eliminated:

$$\begin{aligned} d\Pi_t &= \left( V_t + \mu S V_S + \frac{1}{2} \sigma^2 S^2 V_{SS} \right) dt + \sigma S V_S dW_t - V_S(\mu S dt + \sigma S dW_t) \\ &= \left( V_t + \frac{1}{2} \sigma^2 S^2 V_{SS} \right) dt. \end{aligned}$$

Since the portfolio is locally riskless (no  $dW_t$  term), in an arbitrage-free market it must earn the risk-free rate  $r$ :

$$d\Pi_t = r\Pi_t dt = r(V - SV_S) dt.$$

Equating drifts,

$$V_t + \frac{1}{2} \sigma^2 S^2 V_{SS} = r(V - SV_S).$$

Rearranging, we obtain the Black–Scholes–Merton PDE

$$V_t + \frac{1}{2} \sigma^2 S^2 V_{SS} + rSV_S - rV = 0.$$

### A.3 Proof of the Risk-Neutral Pricing Formula

We now justify the risk-neutral pricing representation

$$V_t = e^{-r(T-t)} \mathbb{E}^{\mathbb{Q}}[g(S_T) | \mathcal{F}_t],$$

where  $g(S_T)$  is the payoff at time  $T$ ,  $r$  is the (constant) risk-free rate, and  $\mathbb{Q}$  is a risk-neutral (equivalent martingale) measure.

*Proof.* Assume a frictionless, arbitrage-free market with a money market account  $B_t = e^{rt}$  and stock price process  $(S_t)_{t \geq 0}$ . By the fundamental theorem of asset pricing, there exists an equivalent probability measure  $\mathbb{Q}$  such that all discounted asset prices are martingales under  $\mathbb{Q}$ . In particular, the discounted stock price

$$\tilde{S}_t := e^{-rt} S_t$$

is a martingale under  $\mathbb{Q}$ .

Suppose a contingent claim with payoff  $g(S_T)$  can be replicated by a self-financing trading strategy in the stock and bond. Let  $V_t$  denote the value of the replicating portfolio at time  $t$ , so that  $V_T = g(S_T)$  almost surely. The discounted value process

$$\tilde{V}_t := e^{-rt} V_t$$

is then also a martingale under  $\mathbb{Q}$ , because it is a linear combination of discounted asset prices in a self-financing strategy.

Martingale property implies

$$\tilde{V}_t = \mathbb{E}^{\mathbb{Q}}[\tilde{V}_T | \mathcal{F}_t] = \mathbb{E}^{\mathbb{Q}}[e^{-rT} g(S_T) | \mathcal{F}_t].$$

Multiplying both sides by  $e^{rt}$ ,

$$V_t = e^{-r(T-t)} \mathbb{E}^{\mathbb{Q}}[g(S_T) | \mathcal{F}_t].$$

In particular, at time  $t = 0$ ,

$$V_0 = e^{-rT} \mathbb{E}^{\mathbb{Q}}[g(S_T)].$$

Thus, arbitrage-free option prices are given by discounted risk-neutral expectations of the payoff.  $\square$